Workshop on Visualisation in Environmental Sciences (EnvirVis) (2015)
A. Middel, G. Weber, and K. Rink (Editors)

An Interactive Web-Based Geovisual Analytics Tool to Explore Water Scarcity in Niger River Basin

T. L. Lei [1], X. Liang[2], G. Mascaro[1], W. Luo[2], D. White[3], P. Westerhoff[1] and R. Maciejewski[2]

[1]School of Sustainable Engineering & the Built Environment, Arizona State University, U.S.A.
[2]School of Computing, Informatics & Decision Systems Engineering, Arizona State University, U.S.A.
[3]School of Community Resources & Development, Arizona State University, U.S.A.

Abstract

Assessing the needs for adaptation and mitigation strategies to climate change and variability in Niger River Basin is a key for future development in Western Africa. There are two major challenges in terms of the assessment: the first is that future projections in water availability based on the historical trends are hard to assess under uncertainty, and the second is that human activities and population growth play a decisive but very uncertain role in environmental impacts. In order to address both challenges, we have developed a geovisual analytics tool for exploring simulation results under combinations of climate models, climate policies, and future population growth. Moreover, our tool is capable of ensemble-visualization and allows users to explore agreement levels among different climate models to assess future uncertainty.

Categories and Subject Descriptors (according to ACM CCS): I.3.8 [Computer Graphics]: Applications—

1. Introduction

The Niger River is the principal river of West and Central Africa and the third longest river in the continent. Its drainage basin covers 2.27 million km^2 and traverses nine countries: Benin, Burkina Faso, Cameroon, Chad, Côte d'Ivoire, Guinea, Mali, Niger, and Nigeria [AG05]. Almost 100 million people in those countries depend on the Niger River in terms of irrigation, fisheries, livestock herding, drinking water, hydropower generation and navigation. Water management, climate change, and population growth are key problems in the Niger River Basin [OA13]. Previous research shows that future hydrological projections in the context of climate change scenarios are uncertain and that population growth also plays a major role in water resource scarcity [Ker10]. To effectively understand the future of the Niger River Basin and the needs of climate adaptation and mitigation, this study develops a new visual analytics tool to assess the expected impact of climate change and population growth under different future scenarios in the basin.

Scenario analysis is considered to be a very important tool to assess climate change and its relevant policies [vVIK*11], allowing analysts to explore the complex and uncertain future interactions among population growth, greenhouse gas emissions, climate, and ecosystems. This paper integrates climate and population growth models into a unified framework through a geovisual analytics approach, in order to support climate scenario analysis in the Niger River Basin. The proposed framework consists of two major views: the simulation view and the uncertainty view. The simulation view allows analysts to explore simulation results under each combination of climate models, climate policies, and future population growth. The uncertainty view allows users to explore agreement levels among different climate models.

2. Related Work

Climatological data have multiple sources such as climatological stations and climate models, as well as relevant social and environmental data, all of which have associated uncertainties. Visualization has been shown to improve understanding uncertainty in climate studies [PWB*09b, PWH11]. For example, Kaye et al. [KHH12] suggested six guidelines to develop an approach to map climate variables and uncertainty. Brus et al. [BVP13] demonstrated several uncertainty visualization methods in climatological data with interpolation methods, in order to help decision-

DOI: 10.2312/envirvis.20151092

support. Sanyal et al. [SZD*10] presented Noodles, a visualization tool to understand ensemble uncertainty within numerical weather models. Similarly, Potter et al. [PWB*09a] presented Vi-SUS/Climate Data and Analysis Tools (CDAT) to explore ensemble datasets from multiple numeric climate models for uncertainty exploration purposes. In addition to uncertainty visualization in climate models and observations, similar research approaches have been applied to understand the impact of climate change on relevant social and environmental fields, such as global water balance [SCFM03] and rural landscapes [DLS*05]. In this paper, we integrate scenario analysis and uncertainty analysis through a visual analytics approach.

3. System Design

The proposed system integrates climate models and population models into a geovisual analytics tool. It allows analysts to design different future scenarios in terms of water supply and water demand under uncertainty, in order to explore water scarcity in the context of climate change in Niger River Basin. In this section, we will introduce all models implemented to calculate water supply, water demand, and water scarcity, as well as our visual analytics environment.

3.1. Water Supply

Water supply was estimated from outputs of different combinations of Global (GCMs) and Regional (RCMs) Climate Models. These were provided by the Coordinated Regional Climate Downscaling Experiment (CORDEX), a project sponsored by the World Climate Research Program that uses a set of advanced RCMs to dynamically downscale the latest set of GCM climate scenarios and predictions produced within the 5^{th} Coupled Model Intercomparison Project (CMIP5) [GA09]. The GCM-RCM combinations of CORDEX were run in a historical period from 1950 to 2005 and for future climate projections from 2006 to 2100 under the newly developed Representative Concentration Pathways (RCPs) [VEK*11].

We extracted runoff spatial outputs at 44 *km* resolution from five GCM-RCM combinations for the historical period and the RCP45 and RCP85 future emission scenarios. Runoff was aggregated at an annual scale. Since the land surface components of the water cycle simulated by climate models are often affected by bias and different sources of uncertainty [HLP13, e.g.], we performed a simple bias correction of the annual runoff using the mean annual climatological runoff observed at four stream gauge stations (Fig. 1 (b)). Observed discharge records were derived from the Global Runoff Data Centre. The maps of bias-corrected annual runoff were used to estimate the water supply following Vörösmarty et al. [VDGR05]. Specifically, for each pixel, water supply was computed as the sum of the local runoff plus river corridor discharge. The resulting maps of water supply have a resolution of 30 sec and units of $m^3/year$ (as shown in Fig. 1 (b).)

3.2. Water Demand

Water demand can be measured in multiple ways. For example, it can be measured in terms of the liters of water per person needed based on daily usage such as drinking and bathing, or based on usage by different sectors such as agricultural and industrial demand. In this paper, we use the Falkenmark index [Fal89], which is an average regional indicator that measures water demand by the total cubic meters of water per person per year in a region. In this measure, the number of people in a region or cell is directly used as a proxy for water demand. To this end, we have collected and generated historical population data as well as population projections. Historical population density data (in $person/km^2$) is collected from the Gridded Population of the World (GPW) v3 from the Socioeconomic Data and Applications Center (SEDAC), Columbia University, which contains estimations of global population density for 1990, 1995 and 2000 (resampled to 30 arc-second (approx. 1km) resolution).

We projected the spatial distribution of future population through the year 2100 using two different models. The first is an exponential growth model assuming that population in the basin will grow at a given percentage each year. The second model for population projection is based on the Shared Social Path (SSP) population projections of Moss et al. [MEH*10]. The SSP provides the projected total population for each of the basin countries at 5 year intervals until 2100. We have used GIS to overlay a layer of administrative boundary shapefiles extracted from GADM [RHM] with the GPW population density layer. The GPW population density data for 2000 is used as the base case scenario. Each pixel of population density raster is scaled up to form a future prediction based on the ratio between the total population of the target year per SSP to which country the pixel belongs, and the total population of the base year.

3.3. Water Scarcity

Based on the per capita water usage in cubic meters, the water conditions in a pixel can be categorized per Falkenmark [Fal89] as: no stress (greater than 1700), stress (between 1000 and 1700), scarcity (between 500 and 1000), and absolute scarcity (less than 500). To apply the Falkenmark indicator, we (i) calculated the water availability per capita per year as the ratio between water supply and population layers (in $m^3/person\ year$), and (ii) classified the supply demand ratio according to the thresholds of 500, 1000 and 1700 (Fig. 1(c)).

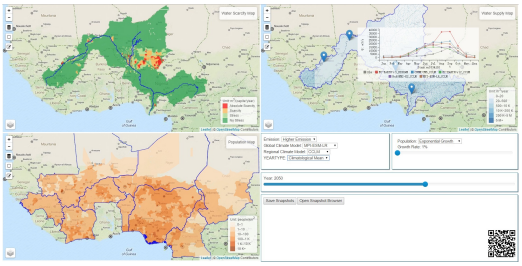

Figure 1: *Simulation view for the RCP85 emission policy with MPI-ESM-LR GCM and CCLM RCM in climatological mean condition in 2050. From top to bottom, and left to right: (a) Water scarcity map in the 4 scarcity levels using Falkenmark indicator, (b) Water supply map with gauge station view and river networks, (c) Water demand map with political boundaries using a 1% exponential growth model, (d) Control panel for composing water scarcity scenarios.*

3.4. Visualization

The goal of our visualization platform is two-fold: 1) to simulate historical and future scenarios, and; 2) to compare and analyze the uncertainty associated with these scenarios. Two visualization views are designed accordingly.

The first view is the simulation view (Fig. 1), which consists of three map panels for geographical information (about water supply, demand, and scarcity, resp.) and one control panel that allows users to enter parameters and generate scenarios. Quantities of water supply and demand were color-coded in an intuitive manner in the map panels. The blue color was used (shown in Fig. 1(b)) to present water supply, and tones from deep blue to light blue represent water supply values from large to small. Similarly, orange colors were used in Fig. 1(c) to represent different levels of water demand. For water scarcity (Fig. 1(a)), four colors: light green, yellow, orange, and red were used to represent increasing levels of water scarcity defined by the Falkenmark index, with alarming colors such as yellow and red indicating areas of scarcity.

In addition to basic information about spatial distributions of water supply and demand, we used interactive visual elements on top of the base layers to provide users with rich information about data, modeling inputs, and spatial contexts. As shown in Fig. 1(b), we have implemented popup windows to visualize the volume of stream flows at stream gauge stations, which were used to derive and calibrate the amount of water supply. Time series of stream flows (m^3/s) by month were plotted as line charts for different climate models.

The control panel (Fig. 1(d)) provides a summary of basic model parameters. Data were organized by the modeling year and then by the types of water demand/supply models. A slide bar and dropdowns were used to allow a user to select any modeling year and combinations of water supply model and demand models. To facilitate decision making and communication in a collaborative environment, we have developed an interface to allow users to store interesting scenarios as model profiles in a database. We have also implemented other features to facilitate data exploration. For example, when exploring maps with dragging or zooming, three maps are synchronized to the same zoom level and view center, which helps in targeting problem areas. Users are also allowed to use an "area selection" mode to highlight regions of interest.

In Fig. 2, following Kaye et al. [KHH12], we used a two-dimensional color matrix that employs color and hue in order to simultaneously visualize the average intensity of water scarcity as predicted by the models as well as uncertainty associated with ensemble predictions using multiple models. The same four colors as in the simulation view were used to represent average water scarcity.

To visualize the uncertainty from ensemble prediction, we introduce the level of agreement among model predictions as a measure of uncertainty. We employ tones as a second channel and use lighter colors to indicate greater uncertainty about an ensemble-predicted water scarcity level. The agreement level is measured as the percentage of the dominant water scarcity value out of all predicted water scarcity values. For example, if 3 out of 5 water demand/supply models predicted "absolute scarcity" for a cell, and the other two predicted "scarcity" and "stress", respectively, the agreement (or certainty) level is $3/5 = 60\%$. In this case, the color of the cell would be salmon red, corresponding to the second column and first row in the legend. By definition, the greater the agreement level, the lower the uncertainty is in an ensemble prediction. We have also explored using an entropy metric to evaluate uncertainty of ensemble prediction as the chaos/entropy in the ensemble of model results, which showed similar spatial patterns of uncertainty as in Fig. 2.

4. Implementation

Our system was implemented using open-source and standards-compliant technology to be maintainable and replicable. GeoServer (hosted in Tomcat server) was used to render geospatial data as a standard Web Mapping Service (WMS), which was consumed by the map engine – the lightweight Leaflet JavaScript library. All data were converted to the GeoTIFF format before being imported into GeoServer. The water scarcity computation was carried out using the GDAL open-source C++ library via its Java interface. The interface and GUI elements were programmed using standard HTML5 and JavaScript, and therefore do not depend on a specific browsers or platform.

5. Case Study

We focus here on the comparisons of water scarcity computed from combinations of five different water supply models under the RCP45 emission scenario and one water demand model (with a 1% exponential growth) as shown in Fig. 2. In total, there are five combinations of water models. We categorize the agreement level into four regions: 40%, 60%, 80%, and 100% for each level of water scarcity.

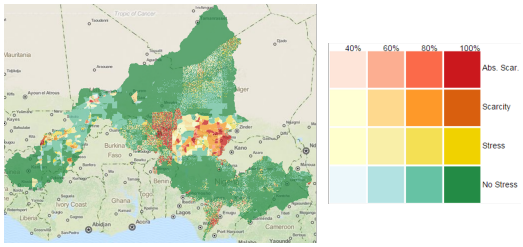

Figure 2: *Agreement view for 5 combinations of water models in 2025. Color matrix (right) shows the visualization scheme. Each row represents different levels of water scarcity with color; each column represents different agreement levels (40% to 100%) with hue.*

From Fig. 2, we can observe that under the assumption of relatively mild future population growth (1%), there is little water scarcity (or absolute scarcity) over the majority of in the basin. Notable exceptions are areas around the cities of Niamey and Sokoto (see also a closer view in Fig. 3), where there is significant water scarcity partly due to the much higher population density there. However, from the tones of the color, we can observe that the five models reach low levels of agreement on the water scarcity around the two cities for 2025 projections. This case study exemplifies the uncertainty associated with ensemble predictions that can be explicitly visualized with our tool and can be neglected when only mean values of model results are used. With our tool, we have also identified cases in which the models predict water scarcity with higher levels of agreement over a longer term. As shown in Fig. 3, we can observe that the future trend of water scarcity of the cities Sokoto (pentagram) and Katsina (X-Star) are converging. While some surrounding regions (the lighter red regions) have higher uncertainty in 2025, they are mostly turning into the absolute scarcity category with high certainty in the more distant future.

6. Conclusion

In this paper, we present a visual analytic framework for analyzing water stress or scarcity in the Niger River Basin. Basin-wide water demand and supply as well as derived water scarcity are visualized using interactive maps, which can provide the user with auxiliary information such as the climatological input, population distribution, and geographical

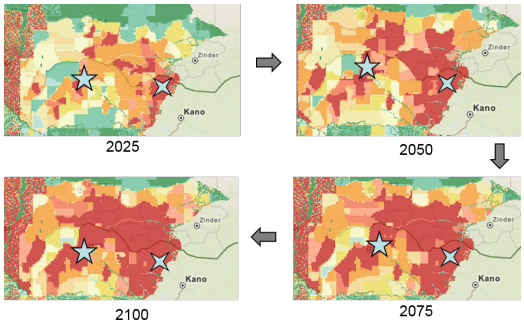

Figure 3: *Converging trend of two cities from 2025 to 2100. The pentagram and X-Star stands for Sokoto and Katsina.*

context within which water scarcity occurs. More importantly, we develop an ensemble visualization tool that facilitates users in exploring different future scenarios by allowing multiple water supply and demand models to be used to predict future patterns of water scarcity.

Acknowledgments

Some material presented here was sponsored by a grant from the Department of Defense and upon work supported by the National Science Foundation under Grant No. 1350573. Disclaimer: The views and conclusions contained herein are those of the authors and should not be interpreted as necessarily representing the official policies or endorsements, either expressed or implied, of ASU, DoD, or the U.S. Government.

References

[AG05] ANDERSEN I., GOLITZEN K. G.: *The Niger river basin: A vision for sustainable management*. World Bank Publications, 2005. 1

[BVP13] BRUS J., VOŽENÍLEK V., POPELKA S.: An assessment of quantitative uncertainty visualization methods for interpolated meteorological data. In *Computational Science and Its Applications–ICCSA 2013*. Springer, 2013, pp. 166–178. 1

[DLS*05] DOCKERTY T., LOVETT A., SÜNNENBERG G., APPLETON K., PARRY M.: Visualising the potential impacts of climate change on rural landscapes. *Computers, Environment and Urban Systems 29*, 3 (2005), 297–320. 2

[Fal89] FALKENMARK M.: The massive water scarcity threatening africa-why isn't it being addressed. *Ambio 18*, 2 (1989), pp. 112–118. 2

[GA09] GIORGI F. C. J., ASRAR G. R.: Addressing climate information needs at the regional level: the cordex framework. *WMO Bulletin 58*, 3 (2009), 175–183. 2

[HLP13] HASSON S., LUCARINI V., PASCALE S.: Hydrological cycle over south and southeast asian river basins as simulated by pcmdi/cmip3 experiments. *Earth System Dynamics 4*, 2 (2013), 199–217. URL: http://www.earth-syst-dynam.net/4/199/2013/, doi:10.5194/esd-4-199-2013. 2

[Ker10] KERRES M.: *Adaptation to Climate Change in the Upper and Middle Niger River Basin*. KfW Entwicklungsbank, 2010. 1

[KHH12] KAYE N., HARTLEY A., HEMMING D.: Mapping the climate: guidance on appropriate techniques to map climate variables and their uncertainty. *Geoscientific Model Development 5*, 1 (2012), 245–256. 1, 3

[MEH*10] MOSS R. H., EDMONDS J. A., HIBBARD K. A., MANNING M. R., ROSE S. K., VAN VUUREN D. P., CARTER T. R., EMORI S., KAINUMA M., KRAM T., ET AL.: The next generation of scenarios for climate change research and assessment. *Nature 463*, 7282 (2010), 747–756. 2

[OA13] OGUNTUNDE P. G., ABIODUN B. J.: The impact of climate change on the niger river basin hydroclimatology, west africa. *Climate Dynamics 40*, 1-2 (2013), 81–94. 1

[PWB*09a] POTTER K., WILSON A., BREMER P.-T., WILLIAMS D., DOUTRIAUX C., PASCUCCI V., JOHHSON C.: Visualization of uncertainty and ensemble data: Exploration of climate modeling and weather forecast data with integrated visus-cdat systems. In *Journal of Physics: Conference Series* (2009), vol. 180, IOP Publishing, p. 012089. 2

[PWB*09b] POTTER K., WILSON A., BREMER P.-T., WILLIAMS D., DOUTRIAUX C., PASCUCCI V., JOHNSON C. R.: Ensemble-vis: A framework for the statistical visualization of ensemble data. In *IEEE International Conference on Data Mining Workshops, 2009. ICDMW'09* (2009), IEEE, pp. 233–240. 1

[PWH11] PÖTHKOW K., WEBER B., HEGE H.-C.: Probabilistic marching cubes. In *Computer Graphics Forum* (2011), vol. 30, Wiley Online Library, pp. 931–940. 1

[RHM] ROBERT HIJMANS NELL GARCIA A. R., MAUNAHAN A.: Gadm database of global administrative areas, version 2.0. http://www.gadm.org. Accessed: 2014. 2

[SCFM03] SLOCUM T. A., CLIBURN D. C., FEDDEMA J. J., MILLER J. R.: Evaluating the usability of a tool for visualizing the uncertainty of the future global water balance. *Cartography and Geographic Information Science 30*, 4 (2003), 299–317. 2

[SZD*10] SANYAL J., ZHANG S., DYER J., MERCER A., AMBURN P., MOORHEAD R. J.: Noodles: A tool for visualization of numerical weather model ensemble uncertainty. *IEEE Transactions on Visualization and Computer Graphics 16*, 6 (2010), 1421–1430. 2

[VDGR05] VÖRÖSMARTY C. J., DOUGLAS E. M., GREEN P. A., REVENGA C.: Geospatial indicators of emerging water stress: An application to africa. *Ambio 34*, 3 (2005), pp. 230–236. 2

[VEK*11] VUUREN D., EDMONDS J., KAINUMA M., RIAHI K., THOMSON A., HIBBARD K., HURTT G., KRAM T., KREY V., LAMARQUE J.-F., MASUI T., MEINSHAUSEN M., NAKICENOVIC N., SMITH S., ROSE S.: The representative concentration pathways: an overview. *Climatic Change 109*, 1 (2011), 5–31. 2

[vVIK*11] VAN VUUREN D. P., ISAAC M., KUNDZEWICZ Z. W., ARNELL N., BARKER T., CRIQUI P., BERKHOUT F., HILDERINK H., HINKEL J., HOF A., ET AL.: The use of scenarios as the basis for combined assessment of climate change mitigation and adaptation. *Global Environmental Change 21*, 2 (2011), 575–591. 1